

## Thermal and Spectroscopic Studies on AgTlSO<sub>4</sub>

S. Rama Rao<sup>1</sup>, D. Rajesh<sup>2</sup>, Ch. Bheema Lingam<sup>3</sup>,  
R.P. Vijayalakshmi<sup>1</sup> and C. S. Sunandana<sup>2\*</sup>

<sup>1</sup>Department of Physics, College of Sciences,  
Sri Venkateswara University, Tirupati 517502,

<sup>2</sup>School of Physics and <sup>3</sup>ACRHEM, University of Hyderabad,  
Hyderabad 500 046, INDIA.

\*Corresponding Author: [sunandana@gmail.com](mailto:sunandana@gmail.com)

### Abstract

AgTlSO<sub>4</sub>, synthesized by mixing Ag<sub>2</sub>SO<sub>4</sub> and Tl<sub>2</sub>SO<sub>4</sub> (1:1 ratio) is characterized by XRD to possess a orthorhombic structure submitted monovalent double sulphate. Thermal characteristics by DSC of AgTlSO<sub>4</sub> shows peaks at 459.7<sup>0</sup>C, 505.4<sup>0</sup>C, 503.4<sup>0</sup>C and 520<sup>0</sup>C that could be attributed to several phase transition from ordered to disordered structure. Raman spectra of AgTlSO<sub>4</sub> exhibit small triplets ( $\nu_3$ ) at about 1085 and 1080 cm<sup>-1</sup> respectively, intense singlets ( $\nu_1$ ) at 953 cm<sup>-1</sup> for Tl derivatives and 968 cm<sup>-1</sup> for Ag derivative very small triplets ( $\nu_4$ ) at about 605 and 615 cm<sup>-1</sup> and medium doublets near 450 cm<sup>-1</sup> which indicates a multiplicity of Z=2, the new spectroscopic unit-cell consisting of two SO<sub>4</sub> ions. ESR gain is due to CO<sub>3</sub><sup>-</sup> radicals and the corresponding g value is 2.365. The g- anisotropy of the CO<sub>3</sub><sup>-</sup> is quite sensitive to the surroundings in which it is stabilized.

### Introduction

A number of solids undergo solid-solid phase Transitions accompanied by a sharp jump in ionic Conductivity in the high temperature phase [1-13]. The conductivity  $\log(\sigma T)$  versus  $T^{-1}$  plot for these solids, e.g. alkali sulphates, Ag<sub>2</sub>SO<sub>4</sub>, AgI, Li<sub>2</sub>MCl<sub>4</sub> spinels, resembles the site percolation probability function, i.e. P(p) plot [14-21], suggesting the percolation model for ion transport in these compounds. The discontinuity in ionic conductivity profile accompanying the solid-solid phase change provides another avenue to probe the mechanism of ion transport. Also the conductivity profile can provide an insight into the mechanism of the structural change occurring during the phase transition. The mixed sulphates - AgLiSO<sub>4</sub>, NaLiSO<sub>4</sub>, RbAgSO<sub>4</sub>, KLiSO<sub>4</sub> and AgTlSO<sub>4</sub> with two monovalent cations are known

to be good solid electrolytes. Some of these compounds exhibit ferroelectric and ferroelastic properties [19]. Due to large polarisability of  $Tl^+$ ,  $Ag^+$ , and  $Rb^+$  cations, Raman scattering can provide information about the local structure and the static or dynamic disorder prevailing in both host frame work and conducting ions sublattice [20]. Fast  $-ion$  conduction in solids has been considered a paradigm for a structure-property relation. The sharp jump in ionic conductivity, up to a factor of  $10^4$ , accompanying the structural change at the phase transition is consistent with this relation. The structure factor can involve coordination geometry number, face-sharing sites and lattice disorder. On the other hand non-structural factors can also contribute significantly such as activated ion concentration, ion-ion interaction or bonding characteristics, vibration amplitudes of neighbouring ions, lattice compressibility or resiliency, ion size, polarisability of the oppositely charged ion and rotational motion of sulphate ions. An assessment of the relative contributions by these factors will provide a better understanding of the transport mechanism [21].  $AgTiSO_4$  and  $RbAgSO_4$  compounds undergo phase transitions at about 440 C (713 K) and 190 C (463 K) respectively to high conducting state [18].  $Tl^+$  ions are known to react very fast with hydrated electron producing  $Tl^0$ . The  $Tl^0$  species is in equilibrium with  $Tl_2^+$  and subsequently forms thallium clusters ( $Tl_n$ ) on further irradiation. Radiolytic reduction of  $Ag^+$  ions in the aqueous medium is one of the most extensively studied systems among the different metal ions. Various transient intermediates such as  $ag^0$ ,  $Ag^{2+}$ ,  $Ag_3^{2+}$ ,  $Ag_4^{2+}$  etc, have been characterized by the technic of pulse radiolysis, and finally results in larger silver clusters with development of plasmon absorption band at  $\sim 380-400$  nm [22]. In this work the thermal and spectroscopic properties of  $AgTiSO_4$  synthesized by a novel mechanochemical method developed earlier by Bharati Mohan and Sunandana [23].

## Experimental

### Synthesis

The material used in this experiment was  $Ag_2SO_4$  (AR 99% pure) and  $Tl_2SO_4$  ALDRICH (99.9%) have been mixed in 1:1 ratio and grinded for one hour in a agate mortar and then transferred to heater. The powder is heated at  $200^\circ C$  for 10 hours, and subsequently cooled to room temperature.  $AgTiSO_4$  was again thoroughly grinded and used for further characterization.

### Instrumentation

The crystal structure of  $AgTiSO_4$  samples is characterized by X-ray powder diffractometer using  $Co\ K\alpha$  radiation ( $\lambda = 1.7889\text{ \AA}$ ). To analyse the morphologies and chemical composition of these samples were obtained by Field emission scanning microscopy (FESEM) and for chemical composition using energy dispersive X-ray scattering (EDS) analysis (a model no ULTRA- 55, ZEISS, Japan). Raman spectra recorded at 300k in a backscattering geometry with Horiba Jobin Yvon, LabRAM-HR800 micro-Raman system using 514.5 nm excitation from  $Ar^+$  gas laser. The differential scanning calorimetry (DSC) was done using DuPont 9900 model DSC instrument. Finally, the electron spin resonance spectra recorded on a JEOL (FE-3X)

x-Band spectrometer under optimized conditioned of modulation amplitude, receiver gain, time constant and scan time.

## Results and Discussion

### Structure and morphology

The XRD pattern of AgTiSO<sub>4</sub> is shown in Fig 1A, The experimental and theoretically obtained XRD of AgTiSO<sub>4</sub> have more or less similar signature. Orthorhombic phase with a space group of Pnam (structure of TiLiSO<sub>4</sub>) has taken as input structure for AgTiSO<sub>4</sub>. After optimization, the structure has been modified and resulting to same as TiLiSO<sub>4</sub>. The obtained 2θ values of XRD pattern matches well with the standard data (JCPDS card no.50-0611 ). The lattice parameters are within orthorhombic symmetry, and the atomic positions are distorted due to the replacement of Li atoms with Ag atoms. This is may be due the mismatch of atomic sizes of Li/Ag atoms. The crystal structure and density of states of AgTiSO<sub>4</sub> as shown in Fig 2. AgTiSO<sub>4</sub> has a band gap of 2.85 eV indicating it is an insulator. This gap is less compared to other sulphates. The optimised lattice parameters and the atomic coordinates obtained from GGA values of AgTiSO<sub>4</sub> along with LiTiSO<sub>4</sub> are shown in table 1 and 2. The nano regime of AgTiSO<sub>4</sub> were observed in FESEM to investigate the morphology and surface characteristics. This sample shows nano particle with average size of the particle is ~80 nm as shown in Fig.1B. The elemental analysis of AgTiSO<sub>4</sub> sample was determined by using EDS technique. The EDS clearly shows the formation of Ti, Ag, O and S elements, formation of AgTiSO<sub>4</sub> and the EDS analysis confirms that the chemical composition of AgTiSO<sub>4</sub> is almost in stoichiometric ratios.

**Table.1:** The optimised lattice parameters obtained from GGA values of AgTiSO<sub>4</sub> along with LiTiSO<sub>4</sub>

Parameters	AgTiSO <sub>4</sub>	LiTiSO <sub>4</sub>
a (Å)	9.301409	8.893
b (Å)	9.628723	9.348
c (Å)	5.902327	5.387
V(Å <sup>3</sup> )	528.616464	447.9

**Table.2:** The atomic coordinates obtained from GGA calculations of AgTiSO<sub>4</sub> and

Atoms	AgTiSO <sub>4</sub>			LiTiSO <sub>4</sub>		
	x/a	y/b	z/c	x/a	y/b	z/c
Ag/Ti	0.318878	0.427416	0.230289	0.495208	0.218639	0.745971
Li/Ti	0.501460	0.227482	0.722854	0.322172	0.412074	0.245216
S	0.220113	0.078072	0.251392	0.207435	0.079567	0.245553
O (1)	0.068945	0.114173	0.314122	0.041108	0.093221	0.250113
O (2)	0.284913	0.188921	0.107915	0.275100	0.214654	0.149477
O (3)	0.306477	0.061271	0.466860	0.264212	0.050570	0.502670
O (4)	0.223651	-0.058058	0.125368	0.252223	-0.042030	0.079800

### Raman Spectroscopy and phase transition

The obtained Raman spectroscopy has shown in Fig.3A. Raman spectra confirms the existence of either a stable or metastable sequence for thallium derivatives. AgTlSO<sub>4</sub> samples exhibit spectra with small triplets ( $\nu_3$ ) at about 1085 and 1080 cm<sup>-1</sup> respectively, intense singlets ( $\nu_1$ ) at 953 cm<sup>-1</sup> for Tl derivatives and 968 cm<sup>-1</sup> for Ag derivative very small triplets ( $\nu_4$ ) at about 605 and 615 cm<sup>-1</sup> and medium doublets near 450 cm<sup>-1</sup> which indicates a multiplicity of Z=2, the new spectroscopic unit-cell consisting of two SO<sub>4</sub> ions[7]. We observed 91cm<sup>-1</sup> as  $\nu_{ext}$ . The intense peak at 956 cm<sup>-1</sup> is denoted as  $\nu_1$ , whereas 435cm<sup>-1</sup> is under the  $\nu_2$  band. The peak 1164 cm<sup>-1</sup> as  $\nu_3$  band.

### Electron spin resonance

Electron spin resonance is a specific microscopic probe with which to examine molecular environments in crystalline and disordered systems. Under favourable circumstances, it is possible to create and stabilize paramagnetic radicles which may reflect certain aspects of dynamics- which may be characteristic of the system itself. Presently we describe our efforts to stabilize and identify molecular paramagnetic radicles in AgTlSO<sub>4</sub>. ESR spectra of AgTlSO<sub>4</sub> consists of an anisotropic resonance (see Fig.3B). This resonance is gain due to CO<sub>3</sub><sup>-</sup> radicals and the corresponding g value is 2.365. The g- anisotropy of the CO<sub>3</sub><sup>-</sup> is quite sensitive to the surroundings in which it is stabilized. This is a strong indirect microscopic evidence in support of the stabilization of the dynamical disorder of SO<sub>4</sub><sup>2-</sup>.

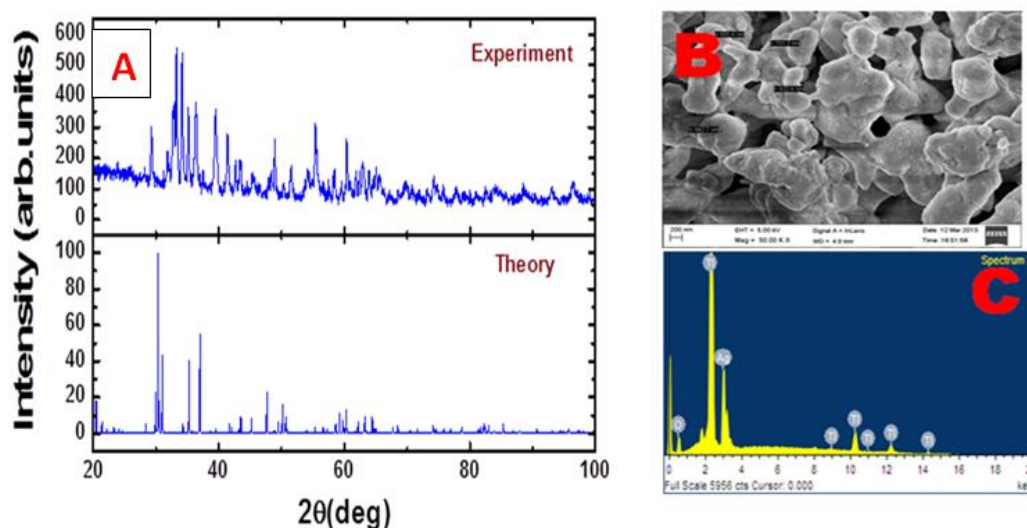
### Differential Scanning calorimetry

Fig.3C shows the DSC scan of the material AgTlSO<sub>4</sub> in the temperature range 50 to 550 °C. The DSC curve of AgTlSO<sub>4</sub> shows small water peak at 184.6°C. An endothermic peaks at 459.7°C, 505.4°C, 503.4°C and 520°C respectively. The endothermic peaks could be due to the phase transition from ordered to disordered low temperature structure. The first endothermic is less intense compared to other endothermic peaks at 503.4°C and 520°C. But there is a strong endothermic peak at 505.4°C. As is common with hydrated systems, these peaks represent dehydration of AgTlSO<sub>4</sub>.

### Fourier Transform Infrared Spectroscopy

In order to get some structural information of AgTlSO<sub>4</sub> solid solution, IR absorption spectra of a mechanically mixed powder of AgTlSO<sub>4</sub> sample are shown in Fig.3D. The free sulphate SO<sub>4</sub><sup>2-</sup> ion belongs to the high symmetry point group. For the four fundamental internal vibration modes, the symmetric stretching mode  $\nu_1$  and the doubly degenerate symmetric bending mode  $\nu_2$  are IR inactive; the asymmetric stretching mode  $\nu_3$  and  $\nu_4$  are both triply degenerate and IR active. In crystalline solids, the sulphate group is influenced by its structural environment. As the symmetry lowers, the degeneracy in  $\nu_2$ ,  $\nu_3$ , and  $\nu_4$  may be expected to be wholly or partially removed and  $\nu_1$  and  $\nu_2$  may become i.r. active. The new phase shows an increase of i.r. transmission, inactive absorption  $\nu_1$  around 597.26 cm<sup>-1</sup> and  $\nu_2$  around 1052.05 cm<sup>-1</sup>. More over the broadening of the i.r. active absorption  $\nu_3$  around

$1112.33\text{ cm}^{-1}$  and  $\nu_4$  around  $624.66\text{ cm}^{-1}$  indicates the decrease in symmetry of the  $\text{SO}_4^{2-}$  ions due to the incorporation of  $\text{Li}^+$  ions in to the interstitial positions and/or  $\text{Ag}^+$  lattice sites, resulting in the change of structural environment. That is, IR spectra indirectly demonstrate the formation of  $\text{AgTlSO}_4$  phase.



**Fig.1.** The(A) X-ray diffraction, (B) FESEM and (C) EDS of  $\text{AgTlSO}_4$ .

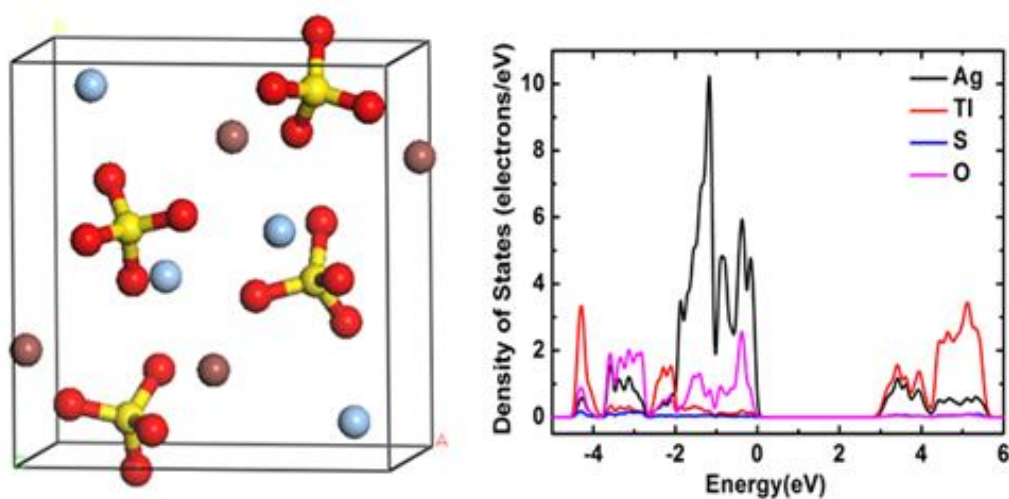


**Fig.2.** The (A) Crystal structure (B) Density of states of  $\text{AgTlSO}_4$

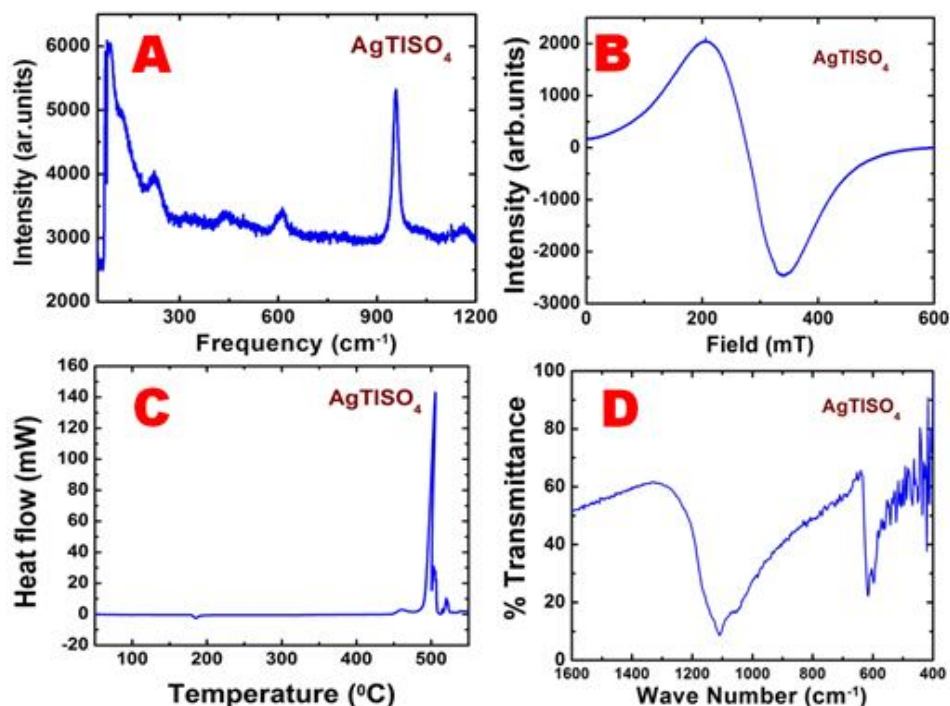


Fig.3. (A) Raman spectroscopy, (B)ESR, (C) DSC and (D) FTIR of AgTiSO<sub>4</sub>

## Conclusions

AgTiSO<sub>4</sub>, is prepared by mixing Ag<sub>2</sub>SO<sub>4</sub> (AR 99% pure) and Ti<sub>2</sub>SO<sub>4</sub>ALDRICH (99.9%) with 1:1 ratio and grinded for one hour. The obtained XRD pattern is in well agreement with the previous studies. Raman spectra of AgTiSO<sub>4</sub> exhibit small triplets ( $\nu_3$ ) at about 1085 and 1080 cm<sup>-1</sup> respectively, intense singlets ( $\nu_1$ ) at 953 cm<sup>-1</sup> for Ti derivatives and 968 cm<sup>-1</sup> for Ag derivative very small triplets ( $\nu_4$ ) at about 605 and 615 cm<sup>-1</sup> and medium doublets near 450 cm<sup>-1</sup> which indicates a multiplicity of Z=2, the new spectroscopic unit-cell consisting of two SO<sub>4</sub> ions. ESR gain is due to CO<sub>3</sub><sup>-</sup> radicals and the corresponding g value is 2.365. The g- anisotropy of the CO<sub>3</sub><sup>-</sup> is quite sensitive to the surroundings in which it is stabilized. The DSC curve of AgTiSO<sub>4</sub> shows small water peak at 184.6°C. An endothermic peaks at 459.7°C, 505.4°C, 503.4°C and 520°C respectively. The endothermic peaks could be due to the phase transition from ordered to disordered low temperature structure.

## References

- [1] Zengcai, L.; Wujun, Fu.; Andrew Payzant E.; Xiang, Y.; Zili, Wu.; Nancy J. D.; Jim, K.; Kunlun, H.; Adam J. R.; Chengdu, L.; *J. Am. Chem. Soc.*, 2013, 135, 975–978.

- [2] Yusheng, Z.; Luke L. D.; *J. Am. Chem. Soc.*, 2012, *134*, 15042–15047.
- [3] Hisashi, K.; Kazushige, O.; Kunihito, K.; *Inorg. Chem.*, 2012, *51*, 9259–9264.
- [4] Radhakrishnan A. N.; PrabhakarRao, P.; Mahesh, S. K.; VaisakhanThampi D. S.; Peter, K.; *Inorg. Chem.*, 2012, *51*, 2409–2419.
- [5] Molenda, J.; *Func. Mat. Lett*, 2011, *4*, 107-112.
- [6] Xin-Xing, Z.; Min L.; *J. Phys. Chem. Lett.*, 2013, *4*, 1205–1210.
- [7] Singh, K.; Bhoga, S. S.; *Bull. Elctrochem.* 1996, *12*, 633-642.
- [8] H. Kasano, S. Tsuchiyama, Y. Kawamura, H. Mashiyama, *Ferroelectrics*, 1998, *217*, 121-128.
- [9] H. Mashiyama, J. Wu, F. Shimizu and M. Takashige, *Physical society of Japan* 1998, *67*, 359-360.
- [10] C. Ramasastry, C.S. Sunandana, B.S.V.S.R. Acharyulu, *J Nonmetals*, 1972, *1*, 283-290.
- [11] Y. Lu, E.A. Secco *Solid State Ionics* 53-56, 223 (1992).
- [12] A. Elfakir, J. Souron, G. Wallez, M. Quarton, M. Touboul, *Solid State Ionics*, 1998, *110*, 145-151.
- [13] R. A. Secco, E. A. Secco, *J. Phys. Chem. Solids*, 1995, *56*, 1045-1051.
- [14] MS Kumari and E A Secco, *Can J Chem* 61 599, 2804(1983).
- [15] KG MacDonald, C MacLean and EA Secco, *Can J Chem* 66, 3132(1988)
- [16] J Olsard, *J Non-CrysI Solids* 1, 235, (1969)
- [17] M D Ingram and C T Moynihan, *Solid State Ionics* 6, 303(1982).
- [18] Yanjia Lu and EA Secco *Solid State Ionics* 53-56, 223-228(1992).
- [19] Y.Lu and E.A Secco *J.Solid State Chemistry* 114, 271(1995).
- [20] S Servagent and PhColomban *Solid State Ionics* 70/71, 167-175(1994).
- [21] E A Secco Richard A Secco *Solid State Ionics* 86-88, 147-154(1996).
- [22] Butler. J, Henglei A *Radiat. Phys. Chem* 15, 603-612 (1980).
- [23] D. Bharati Mohan, C.S. Sunandana *J. Phys. Chem. Solids* 67, 2583 (2006).

